

OH main line masers in the M82 starburst

M.K. Argo, A. Pedlar, R.J. Beswick, T.W.B. Muxlow

University of Manchester, Jodrell Bank Observatory, Macclesfield, Cheshire SK11 9DL

7 December 2018

ABSTRACT

A study of the distribution of OH gas in the central region of the nearby active starburst galaxy M82 has confirmed two previously known bright masers and revealed several new main line masers. Three of these are seen only at 1665 MHz, one is detected only at 1667 MHz, while the rest are detected in both lines. Observations covering both the 1665 and 1667 MHz lines, conducted with both the Very Large Array (VLA) and the Multi-Element Radio Linked Interferometer Network (MERLIN), have been used to accurately measure the positions and velocities of these features. This has allowed a comparison with catalogued continuum features in the starburst such as HII regions and supernova remnants, as well as known water and satellite line OH masers. Most of the main line masers appear to be associated with known HII regions although the two detected only at 1665 MHz are seen along the same line of sight as known supernova remnants.

Key words: masers - galaxies: individual: M82 - galaxies: ISM - galaxies: starburst

1 INTRODUCTION

Astronomical masers are useful probes of the interstellar medium in star forming regions, both in the Milky Way and external galaxies. Masers usually occur under specific conditions found in star forming regions so the presence of a maser immediately provides information on the state of the ISM and acts as an indicator for ongoing star formation.

Studies of star forming regions within the Milky Way have the advantage that the masers can be studied at high linear resolution. In our own Galaxy, OH masers have typical luminosities of 2×10^{21} Watts and sizes of 2 to 20 AU (Minier et al. 2002). At the other end of the scale are the so-called megamaser sources in active galaxies, sources a factor of 10^7 brighter than ordinary Galactic masers, such as that discovered in Arp220 (IC 4553; Baan et al. 1982). In between these extremes of the phenomenon are masers such as those detected previously in M82 (Weliachew et al. 1984). These have observed intensities of $\sim 10^{25}$ Watts and are sometimes referred to as “kilomasers” (e.g. Hagiwara et al. 2001; Henkel & Wilson 1990). Studies of kilomaser sources in individual galaxies, such as M82, provides a sample of masers which are all at an approximately equal distance and hence can be observed with the same linear resolution.

This paper describes an investigation into the main line OH maser population in the nearby starburst galaxy M82 using data from both the Very Large Array (VLA) and Multi-Element Radio Linked Interferometer Network (MERLIN). The maser population is investigated and their positions and velocity distribution are compared to other known objects and the distribution of other gases.

Telescope used	Date of observation	Angular resolution	Bandwidth	Velocity resolution
MERLIN	1995 Nov.	0''2	8 MHz	23 km s ⁻¹
MERLIN	1997 May	0''2	2 MHz	1.4 km s ⁻¹
VLA	2002 Apr/May	1''4	6.3 MHz	18 km s ⁻¹

Table 1. Summary of the observations of OH masers in M82.

2 MASERS IN THE M82 STARBURST

M82 is one of the closest, and therefore best studied, starburst galaxies and radio observations of this galaxy are numerous. Extensive studies of the distribution and dynamics of neutral hydrogen have been made (e.g. Wills et al. 2000, 2002) and these have been compared with the molecular gas as traced by CO emission (Shen & Lo 1995). The angular resolution of the CO observations is, however, comparatively low. Observations of the transitions of the OH molecule can be made with the same instruments at similar resolution to the previous HI studies and so provide a better comparison of atomic and molecular gas.

An OH maser was first detected in M82 using the Effelsberg telescope by Nguyen-Q-Rieu et al. (1976). Using the VLA, Weliachew et al. (1984) detected two main line maser regions in the galaxy and noted that, although both spots are an order of magnitude brighter than the most luminous Galactic maser, the emission from those in M82 may be coming from a number of smaller masers within each spot. The

arXiv:0706.1149v1 [astro-ph] 8 Jun 2007

resolution of these observations however was not sufficient to detect any substructure or extension in either masing region.

Subsequent observations have resulted in further detections of masers at other frequencies. A total of six OH features were detected using the 1612 and 1720 MHz satellite lines by Seaquist et al. (1997). Four features were seen in emission at 1720 MHz, two were seen in absorption at the same frequency, while only one feature was detected in emission at 1612 MHz at the same position as one of the 1720 MHz absorption features. H₂O masers have also been detected in M82 at 22 GHz (Baudry & Brouillet 1996; Hagiwara 2005).

Recently MERLIN and the VLA have been used to probe the OH absorption across the central starburst region in M82. As well as deep absorption features, eleven main line OH masers have been detected to a limit of 3σ , nine of which are new detections.

Unless otherwise stated, all positions are given in J2000 coordinates in the format aa''aaa bb''bb corresponding to 09^h55^maa''aaa and +69°40'bb''bb respectively. At the distance of M82 (3.2 Mpc, Freedman et al. 1994), one arcsecond corresponds to a linear distance of 15.5 parsecs.

3 OBSERVATIONS

Data from the MERLIN archives, as well as more recent VLA observations, have been used to investigate the maser population in M82. A summary of the observations discussed here is given in Table 1 and further details are given in the following Section.

3.1 MERLIN archive

3.1.1 1995 observations

MERLIN observations of OH in M82 were carried out on 26th November 1995 using a total bandwidth of 7.75 MHz over 64 channels giving a velocity resolution of $\sim 22 \text{ km s}^{-1}$ at a wavelength of 18 cm. Eight of the MERLIN telescopes were included in the array for these observations: Lovell, Mk 2, Tabley, Darnhall, Knockin, Defford, Cambridge and Wardle (the Wardle antenna has since been decommissioned). This provided a maximum baseline of 217 km and hence a resolution of $0''.2$ at a wavelength of 18 cm. Gaussian fitting of components using the AIPS task JMFIT resulted in a position uncertainty, relative to the phase calibrator, of $\pm 0''.02$.

This was a preliminary observation intended to detect the two known masers, look for additional sources of OH emission, and also to probe absorption by OH in the central starburst in M82 to provide a comparison with that detected in CO emission (for example). Due to the u - v coverage of MERLIN, however, extended absorption features are resolved out and very little absorption was actually detected in these observations. Several emission features were detected, however. Figure 1 shows spectra of the masers detected in this observation. Table 2 lists the masers found in 1995 MERLIN data together with their positions and flux densities in this data-set. The ID label for each maser, given in column one, is constructed from the VLA 2002 position where known. The exception to this is 50.02+45.8 whose ID is determined from the MERLIN positions listed in Table

ID	RA	Dec	S ₁₆₆₅ (mJy)	S ₁₆₆₇ (mJy)	Ratio
53.11+48.0	53 ^o 094	47''88	5.57	<2.6	<0.47
50.97+45.3	50.924	45.37	8.35	7.83	0.94
50.35+44.1	50.350	44.13	7.01	29.9	4.27
50.02+45.8	50.017	45.83	4.30	5.09	1.18
49.71+44.4	49.689	44.17	<2.6	5.29	>2.03
48.45+42.1	48.360	41.93	4.15	6.94	1.67

Table 2. Definite maser detections made with MERLIN in 1995. The 3σ noise per channel was 2.6 mJy/beam. The IDs are constructed from the J2000 positions measured in the VLA 2002 data-set. The flux densities are given in mJy and the listed ratios are for S₁₆₆₇:S₁₆₆₅.

ID	RA	Dec	S ₁₆₆₅ (mJy)	S ₁₆₆₇ (mJy)	Ratio
50.97+45.3	50 ^o 924	45''37	<18	23.0	<1.35
50.35+44.1	50 ^o 384	44''24	<18	57.3	<3.36

Table 3. Definite maser detections made with MERLIN in 1997. The flux densities are given in mJy and the ratio is S₁₆₆₇:S₁₆₆₅. The 3σ noise was 17 mJy/beam in the 1665 MHz observation and 18 mJy/beam in the 1667 MHz observation.

2 as it was not detected in the 2002 data. Note that the spectra are shown smoothed with a Gaussian of width two channels, while the peak flux densities listed in Table 2 are measured from the unsmoothed data.

3.1.2 1997 observations

These observations were carried out in May 1997 by switching between 1612, 1665, 1667, and 1720 MHz using seven telescopes of the MERLIN array: Defford, Cambridge, Knockin, Darnhall, Mk 2, Lovell and Tabley. The correlator was configured to record 256 frequency channels 7.7 kHz in width, giving a velocity resolution of 1.4 km s^{-1} . Only the 1665 and 1667 MHz observations are discussed here. Figure 2 shows spectra of the two masers detected at 1667 MHz, illustrating the narrower frequency channel widths in this observation. Gaussian fitting components in these data resulted in a position uncertainty of $\pm 0''.03$.

As these observations were carried out using narrower frequency channels than the 1995 observations there is a reduction in sensitivity. The 3σ noise level per channel in these observations was 16.9 mJy/beam at 1665 MHz and 18.2 mJy/beam at 1667 MHz, the difference arising from the longer observation at 1665 MHz.

As stated previously, the u - v coverage of MERLIN is not ideal for detecting extended absorption and most of it was resolved out in these observations. For detecting compact objects such as masers, however, MERLIN's resolution is an advantage as the observations are not greatly affected by deep absorption features.

The detections made in the 1667 MHz data-set are listed in Table 3. No detections were made in the 1665 MHz data-set. In most cases in the other data-sets examined, the masers are significantly weaker in this line compared to the 1667 MHz line.

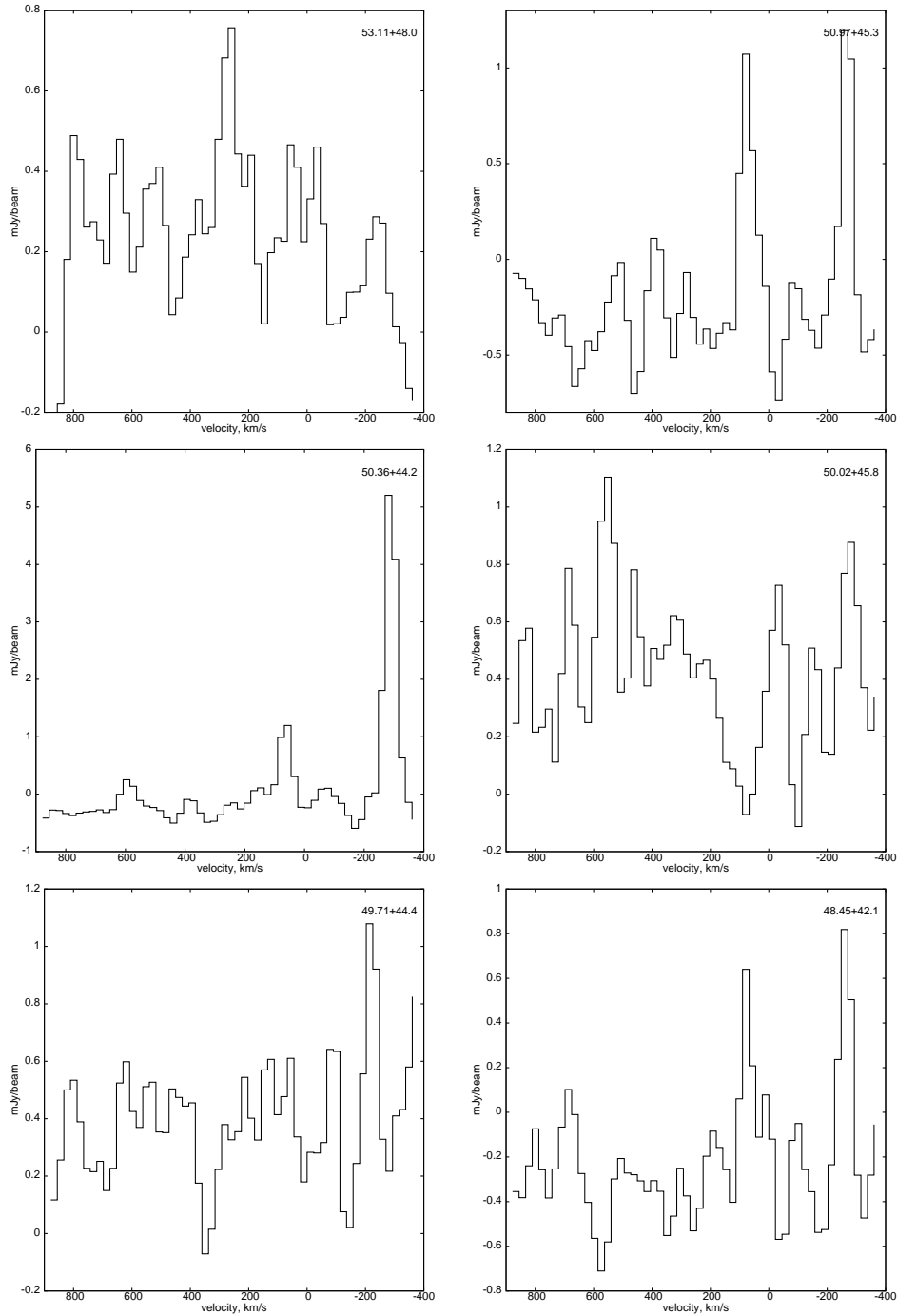


Figure 1. Spectra of the maser features detected in the 1995 observations with MERLIN. All are detected at $>3\sigma$ at least one line. The labels in the top right of each panel correspond to the IDs given in Table 2. The 3σ noise level in each channel is 2.59 mJy/beam and the spectra shown here have been smoothed in frequency using a Gaussian of width two channels. The x -axis velocity scale is calculated relative to the rest frequency of the 1665 MHz line.

3.2 VLA 2002

Observations were carried out in April and May 2002 using the VLA in A configuration. At 1.6 GHz this gives an angular resolution of $\sim 1''.4$. The data were taken in two observing runs, one of which was carried out in April, the other in May 2002. The data were recorded in 64 channels over a bandwidth of 6.25 MHz such that both main line maser frequencies were within the observing band over the

extent of the velocity range within the disk of the galaxy. This setup resulted in a velocity resolution of 18 km s^{-1} . 3C286 (1331+305) was used for flux calibration, 0319+415 was used for bandpass calibration, and the phase calibrator was 0954+745. Calibration of the data was performed using standard techniques for the VLA. In order to isolate the line component, the radio continuum emission was subtracted using a set of line free channels near the start and

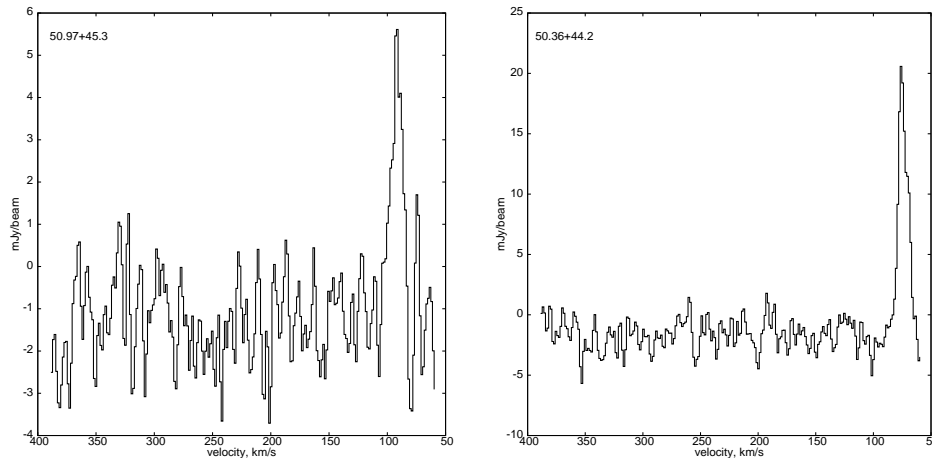


Figure 2. Spectra of the two maser features detected at 1667 MHz in the 1997 observations with MERLIN. The 3σ noise level in each channel was 18.2 mJy/beam. The data are shown smoothed in frequency using a Gaussian of width two channels. The x -axis velocity scale is calculated relative to the rest frequency of the 1667 MHz line.

end of the cube where the channel frequency fell outside that corresponding to the velocity range for OH in M82.

Some of the maser features are bright enough to cause ringing in the 2002 VLA data. This effect can be largely removed by smoothing the data, although this results in adjacent channels no longer being independent. This was carried out using the AIPS task XSMTH to apply a Gaussian function with a width of two channels. This also has the effect of reducing the measured peak flux since the emission is effectively smeared over several channels, hence the peak fluxes listed in Table 4 were measured in the unsmoothed data.

The OH absorption across the central starburst in M82 is well displayed in these observations, but the spectral resolution of the data-set is not ideal for maser studies. Despite this, several maser features were detected in emission in these data. Table 4 lists the positions of the maser features in this data-set which are $>3\sigma$, while Figure 3 shows a plot of the maser positions on top of a contour plot of the OH absorption across the M82 starburst. Gaussian fitting resulted in a position uncertainty of $\pm 0''.2$. Figure 4 shows spectra of each maser feature listed in Table 4.

The criteria used for classifying a signal as a maser was a detection of at least 3σ in two or more consecutive channels. This excludes some features which only appear in a single channel. Due to the wide channels of this observation it is possible that some masers are missed altogether. This could be because the emission is narrow but happens to fall at a channel edge, becoming spread over a couple of channels and hence too close to the noise level to be a firm detection.

Another major factor affecting the detection of a maser signal in these data is the depth of the absorption. As can be seen in Figure 4, some of the masers are coincident with deep absorption features and are only detected because they are very bright. Weaker masers whose brightness is less than the magnitude of the depth of the absorption at the same position are therefore difficult to detect in these observations.

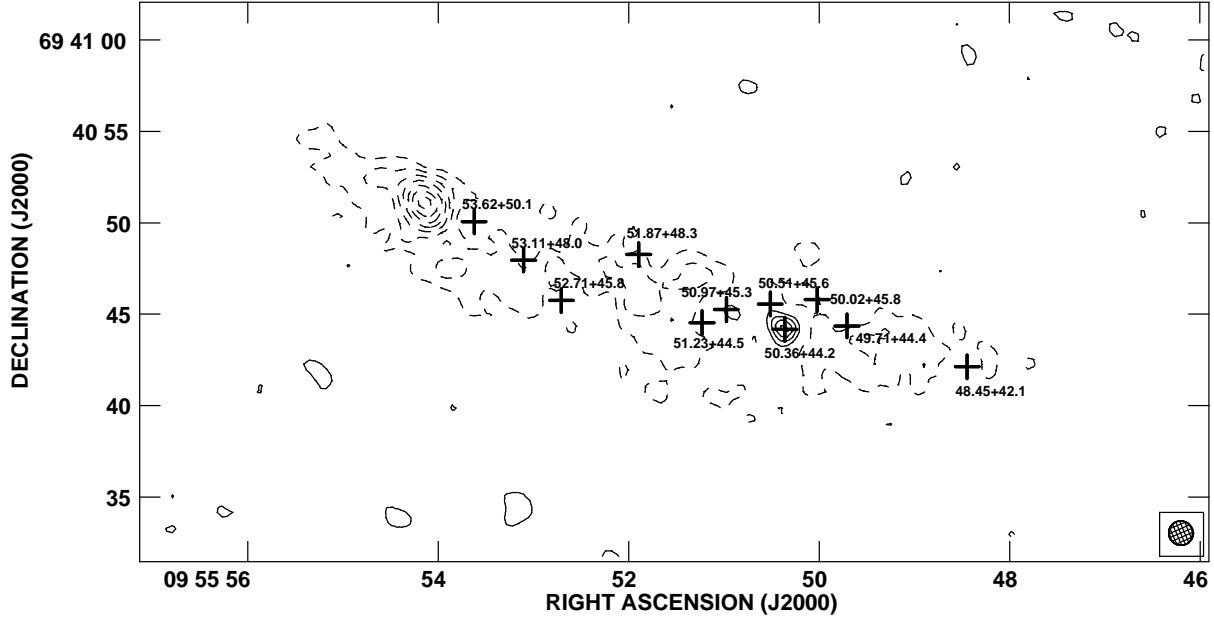


Figure 3. The location of the masers listed in Table 4 superimposed on a contour plot of the OH absorption in the 2002 VLA data cube which has been continuum subtracted and summed in frequency using the AIPS task SQASH. Contours are from -10 to +10 (in steps of $1) \times 0.2 \text{ mJy beam}^{-1}$. Solid contours are positive, dashed contours are negative. The diameter of each symbol is that of the restoring beam, $1''3$.

ID	R.A. (J2000)	Dec. (J2000)	S_{1665} (mJy)	S_{1667} (mJy)	Ratio (1667:1665)
53.62+50.1	53 ^h 647	50 ^m 09	2.44 mJy	2.49 mJy	1.02
53.11+48.0	53.105	47.97	1.86	<0.77	<0.41
52.71+45.8	52.707	45.75	5.02	<0.77	<0.15
51.87+48.3	51.868	48.31	1.71	<0.77	<0.45
51.23+44.5	51.230	44.54	4.85	5.93	1.22
50.97+45.3	50.974	45.27	13.0	18.5	1.42
50.51+45.6	50.513	45.57	1.85	1.28	0.692
50.36+44.2	50.360	44.18	10.7	50.5	4.72
49.71+44.4	49.707	44.37	<0.77	2.34	>3.04
48.45+42.1	48.445	42.13	2.64	5.97	2.26

Table 4. Definite maser detections identified from the VLA 2002 data. Limits on the measured flux densities are given as 3σ . The maser IDs here are constructed from the positions measured in this data-set and are used throughout this paper.

4 NOTES ON INDIVIDUAL SOURCES

A brief description is given here for each source. A more detailed discussion of the properties of the maser population is given in the following section. **Note** that, while the masers are identified here according to their J2000 positions, the continuum features to which they are compared (from McDonald et al. 2002) are identified using the B1950 coordinate convention of Kronberg & Wilkinson (1975).

53.62+50.1 is coincident with an HII region (44.93+63.9) and was detected in both main lines in all but the 1997 data-set.

53.11+48.0 is coincident with a supernova remnant

(44.43+61.9) and, while it was seen at 1665 MHz in all but the 1997 data-set, it was not detected at 1667 MHz in any observation.

52.71+45.8 is coincident with both a supernova remnant (44.01+59.6) and a satellite line maser (feature 4 from Seaquist et al. 1997). Like 53.11+48.0, this maser is not detected at 1667 MHz in any observation. It is detected at 1665 MHz in the 2002 data-set.

51.87+48.3 is apparently not coincident with a known continuum feature or either of the other types of maser shown in Figure 7. This source was only detected in the 2002 data and was one of the weaker detections.

51.23+44.5 is located within an arcsecond of an HII region (42.48+58.4), and close to two water maser features (S1 and P3 from Baudry & Brouillet 1996) and two further HII regions. Despite not being detected in either the 1995 or 1997 observations, it is seen in both lines in 2002.

50.97+45.3 appears coincident with both an HII region (42.21+59.2) and a water maser feature (S2 from Baudry & Brouillet 1996). In the 1997 and 2002 observations this source is brightest at 1667 MHz, however in 1995 it was brighter at 1665 MHz.

50.51+45.6 is not clearly associated with another feature in M82 and is brighter at 1665 MHz than 1667 MHz.

50.36+44.2 is closely associated with an HII region (41.64+57.9) and within a beam width of a water maser (S3 from Baudry & Brouillet 1996). This source is the brightest maser feature in the M82 starburst and is significantly brighter (by a factor of more than four) at 1667 MHz than it is at 1665 MHz, the most extreme line ratio out of all the detections.

50.02+45.8 is located between a supernova remnant (41.29+59.7) and a possible water maser (P2 from Baudry & Brouillet 1996) and is about a beam width from each. It is only detected in the 1995 data-set where it is brightest at 1667 MHz.

49.71+44.4 is coincident with a possible water maser feature (P1 from Baudry & Brouillet 1996) and also within a beam width of two HII regions (40.95+58.8 and 40.96+57.9). It is brighter at 1667 MHz in every data-set in which it is detected, not appearing above the noise in any data-set at 1665 MHz. This maser appears to consist of two closely-spaced velocity components.

48.45+42.1 is also within a beam width of an HII region (39.68+55.6), close to a water maser feature (S4 from Baudry & Brouillet 1996) and is consistently brighter at 1667 MHz.

5 DISCUSSION

5.1 Line ratios

For an optically thin cloud in local thermal equilibrium, the ratio of emission for the ground states (1667:1665:1612:1720) is 9:5:1:1, so $S_{1665} > S_{1667}$ is impossible without excitation such as that provided by a maser pumping mechanism. Table 5 lists the ratios between the two main lines for each maser from the observations discussed here, with limits given (based on the 3σ detection limit) where a detection was made in only one of the two main lines.

In the MERLIN 1995 observations, four of the six

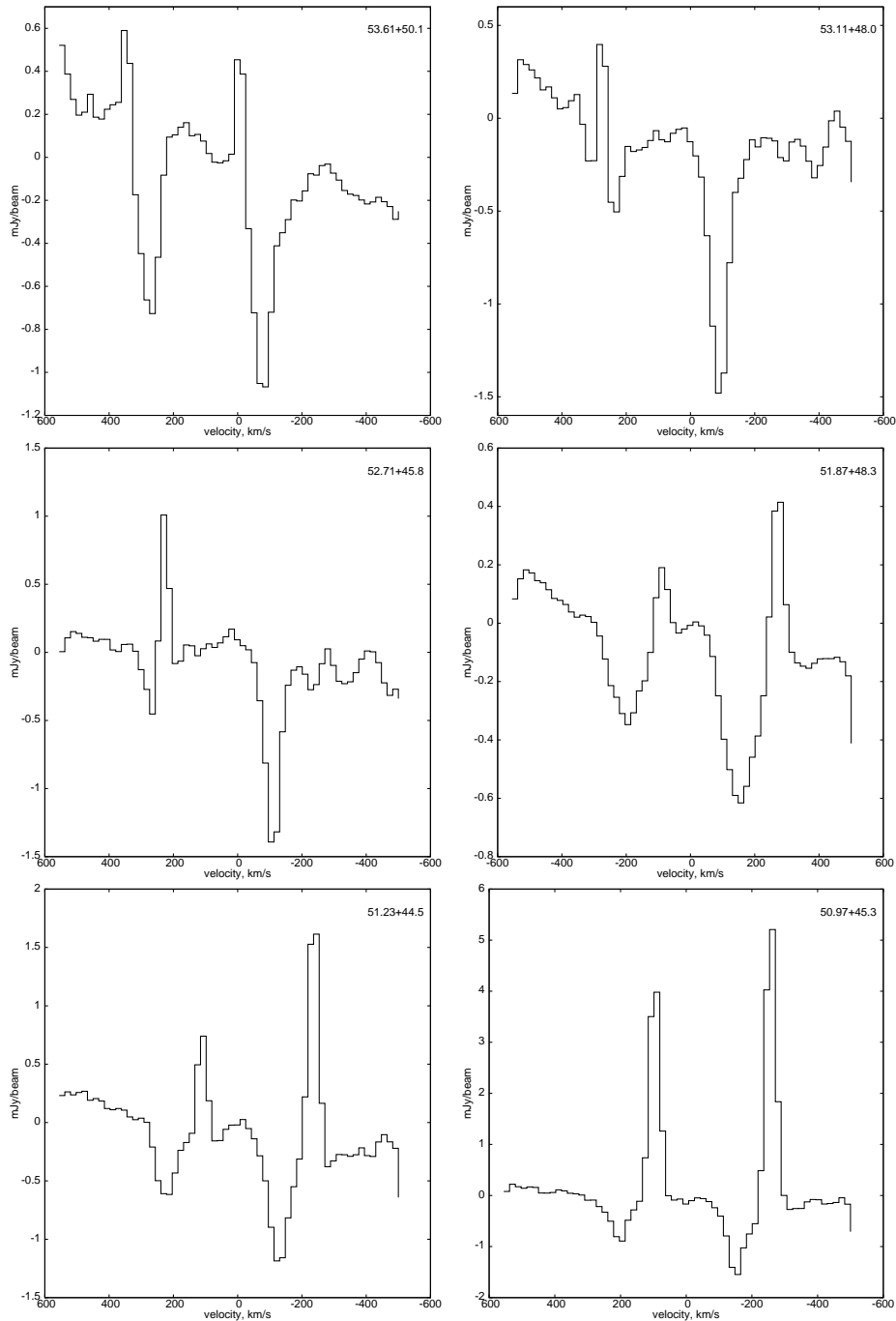


Figure 4. Spectra of each maser listed in Table 4, arranged in order of decreasing R.A. Each maser is seen as two or more adjacent channels with a flux greater than three times the rms noise level. The data are smoothed with a Gaussian of width 2 channels. The x -axis velocity scale is calculated relative to the rest frequency of the 1665 MHz line. Continued on next page.

masers are detected in both main lines, while 53.11+48.0 is detected only at 1665 MHz and 49.71+44.4 is present only at 1667 MHz. In 1997, the two masers detected were seen only at 1667 MHz. In 2002 six of ten are seen in both lines, 53.11+48.0, 52.71+45.8 and 51.87+48.3 are seen only at 1665 MHz, while 49.71+44.4 is again seen only at 1667 MHz.

Of those which appear to be associated with HII regions, most are brighter at 1667 MHz than at 1665 MHz. The only exception to this is 50.97+45.3 which is reversed only in

the 1995 observations. The difference in magnitude between the two lines is, however, less than 1σ . Two of the masers, 53.11+48.0 and 52.71+45.8, appear to be associated with supernova remnants. These two masers are both detected only at 1665 MHz, if they are detected at all, with no emission apparent at 1667 MHz. Further discussion of apparent associations with other known features are given in the next section.

Investigating whether the masers vary in intensity be-

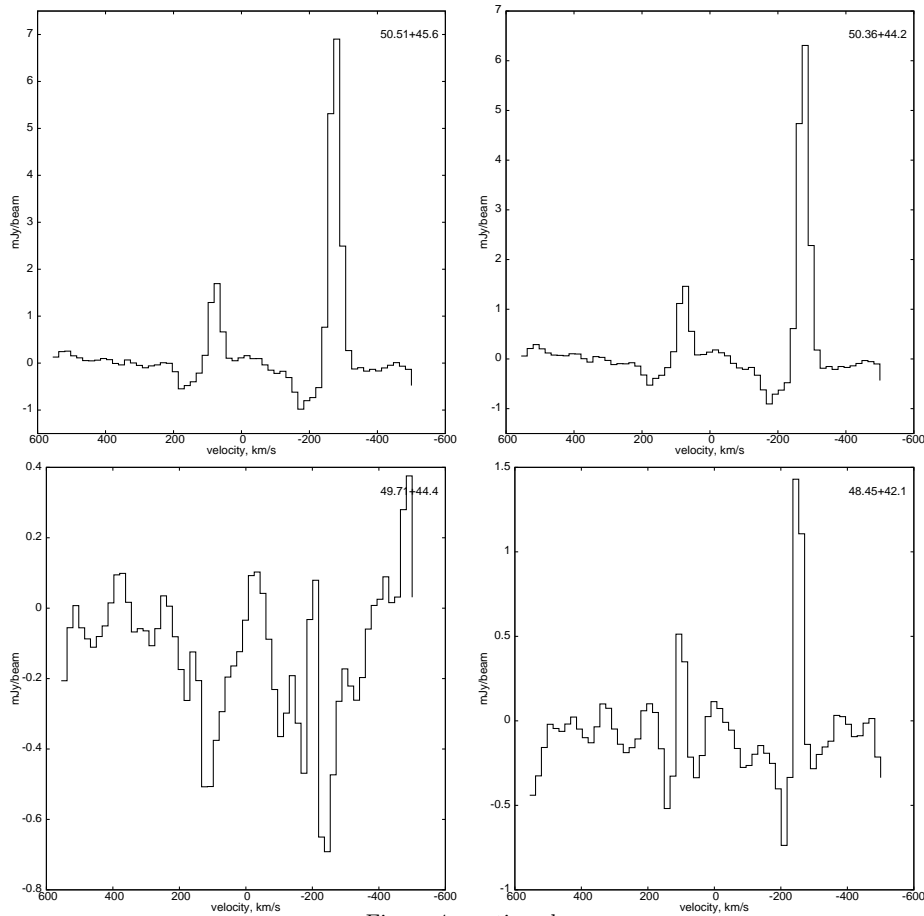


Figure 4: continued.

ID	R ₁₉₉₅	R ₂₀₀₂	Closest feature
53.62+50.1	-	1.02	44.93+63.9 (HII)
53.11+48.0	<0.47	<0.41	44.43+61.8 (SNR)
52.71+45.8	-	<0.15	44.01+59.6 (SNR)
51.87+48.3	-	<0.45	-
51.23+44.5	-	1.22	42.48+58.4 (HII)
50.97+45.3	0.94	1.42	42.21+59.2 (HII)
50.51+45.6	-	0.69	-
50.36+44.2	4.27	4.72	41.64+57.9 (HII)
50.02+45.8	1.18	-	41.29+59.7 (SNR)
49.71+44.4	>2.03	>3.04	40.96+57.9 (HII)
48.45+42.1	1.67	2.26	39.68+55.6 (HII)

Table 5. Ratios of the measured intensities in the 1667 MHz line to the 1665 MHz line for each maser in M82. Limits are given using the measured noise level in each cube. The listed associations are the nearest continuum features (within a beam width of the maser position) from McDonald et al. (2002), labelled according to their B1950 coordinates.

tween the epochs is not as simple as comparing their flux measurements. The different channel widths used in each observation will determine, to some extent, the flux densities measured. An alternative measure is the ratio between the two main line intensities in which the difference in channel width will have the same effect on each of the two lines.

It can be seen from Table 5 that, to within the uncertainties of the flux measurements, all of the ratios are consis-

tent over the different epochs of observation. The limits on the ratio for 49.71+44.4 also vary by an amount larger than the uncertainties in the measured flux densities, with the 1667 MHz line becoming comparatively bright in the 2002 data. This source is interesting as it has additional structure which is apparent in the 2002 observations (see Section 5.5).

One source, 50.02+45.8, was detected in 1995, but is not visible in the 2002 observations. This source is one of the weakest seen in 1995 and may have faded below the noise level in subsequent observations. Several sources appear in the 2002 data-set, but not in the 1995 data. One likely cause of this is due to the width of the channels in the 1995 data-set which will average narrow emission so that it appears weaker, possibly reducing it below the detection threshold. Variability is often observed in Galactic masers (e.g. Caswell et al. 1980), so it is possible that these masers are varying in intensity between observations.

5.2 Associations

Figure 5 shows the positions of both the main line maser detections described here and the SNRs from McDonald et al. (2002). Figure 6 shows the positions of the OH masers along with the HII regions from McDonald et al. (2002). Figure 7 shows the positions of the main line OH masers described here along with the satellite line masers detected by Seaquist et al. (1997), the H₂O masers (both detections

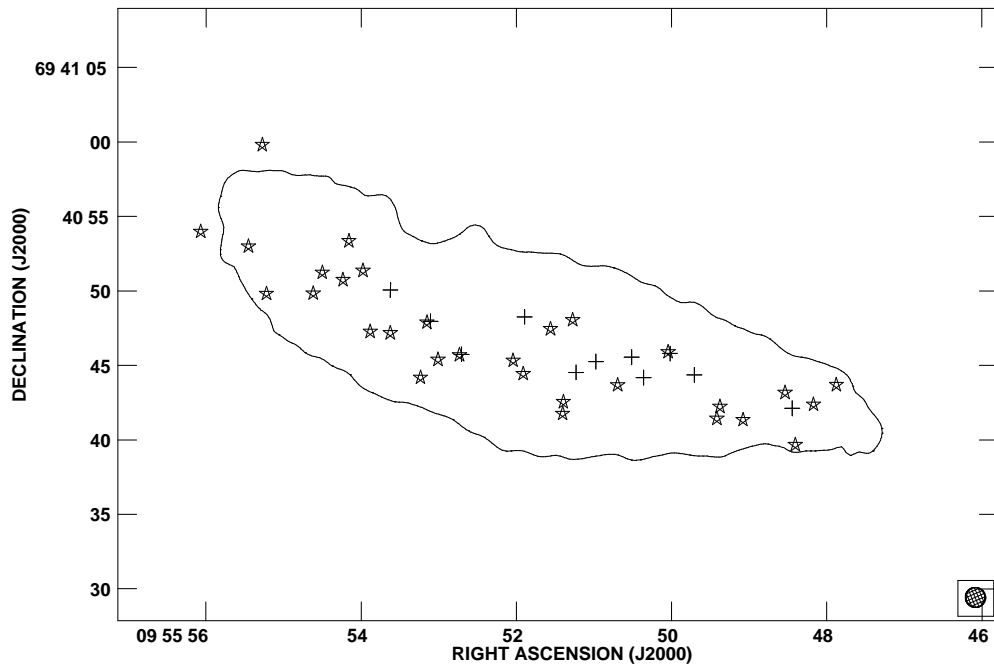


Figure 5. The location of the main line masers (crosses) compared to the supernova remnants from McDonald et al. (2002) (stars). The outline of the galaxy is provided by a $1-\sigma$ contour of the continuum emission at 18 cm.

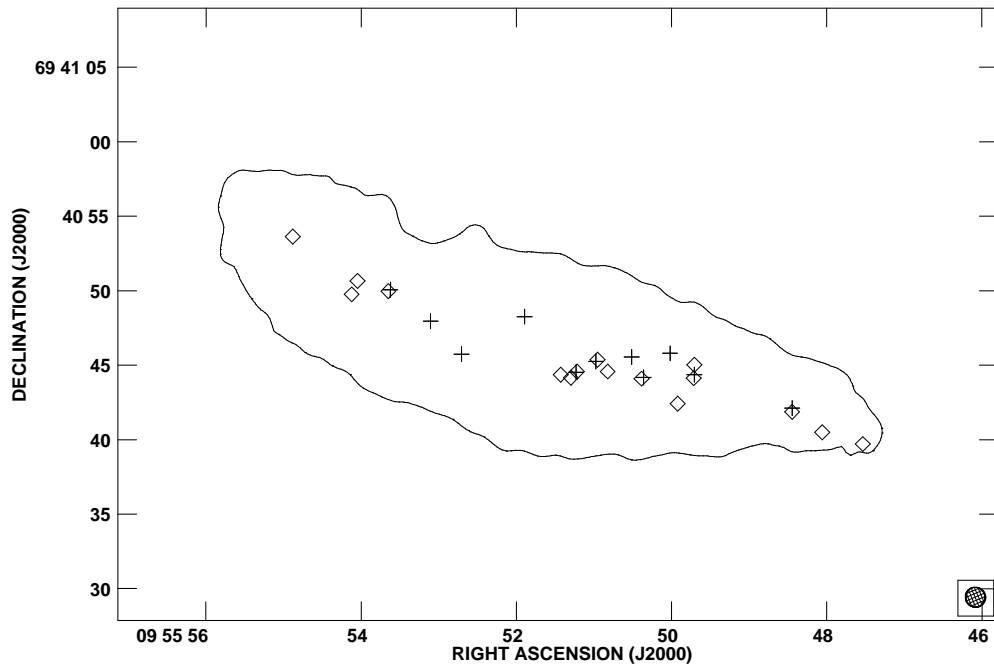


Figure 6. The location of the main line masers (crosses) compared to the HII regions from McDonald et al. (2002) (diamonds). The outline of the galaxy is provided by a $1-\sigma$ contour of the continuum emission at 18 cm.

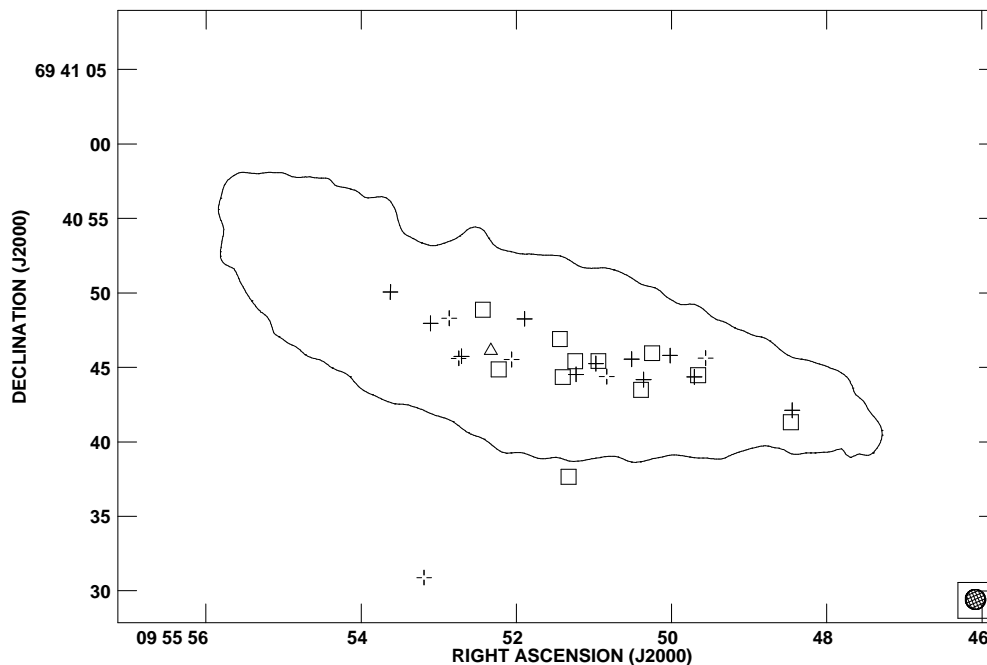


Figure 7. The location of the main line masers (crosses) compared to satellite line masers from Seaquist et al. (1997) (broken crosses), water masers from Baudry & Brouillet (1996) (squares) and the $2.2 \mu\text{m}$ peak from Lester et al. (1990) (triangle). The outline of the galaxy is provided by a $1-\sigma$ contour of the continuum emission at 18 cm.

and possible detections) listed in Baudry & Brouillet (1996) and the $2.2 \mu\text{m}$ peak from Lester et al. (1990). In all three of these figures, the outline of M82 is represented by a 1σ contour from the continuum emission in the VLA 2002 observation. From these figures it can be seen that most of the masers described here are closely associated with other known objects within M82.

Four sources (51.23+44.5, 50.97+45.3, 50.37+44.1 and 48.45+42.1) are all apparently coincident with a water maser feature to within the size of the beam in the VLA 2002 observations. A further two (50.51+45.6 and 49.71+44.4) are located close to possible H_2O maser detections. Of these associations, 50.51+45.6 is the most marginal as the separation is of the order of the beam size. 51.23+44.5 is within a beam of two separate water maser features, one of which is a marginal detection, listed in Baudry & Brouillet (1996).

Only a minority of the main line OH masers described here (four of eleven) do not appear coincident with water maser detections. Of these, all except 51.87+48.3 are coincident with other known features. All of the definite water maser detections listed by Baudry & Brouillet (1996) are coincident with an OH main line maser detected in these observations.

Six OH masers (53.62+50.1, 51.23+44.5, 50.97+45.3, 50.36+44.2, 49.71+44.4 and 48.45+42.1) appear to be associated with HII regions, while three (53.11+48.0, 52.71+45.8 and 50.02+45.8) are within a beam of known supernova remnants. The large number of apparent associations is not surprising given the crowded fields and that maser emission is the result of an amplification of background continuum emission. From the line ratios listed in the previous section it can

be seen that the sources apparently associated with HII regions are generally brighter at 1667 than at 1665 MHz, while those close to supernova remnants are brighter at 1665 MHz (apart from 50.02+45.8). In studies of Galactic masers such as that carried out by Caswell (1998), most masers in star forming regions are found to be brighter at 1665 MHz than at 1667 MHz. This is discussed further in Section 6.

The region around 49.71+44.4 contains two HII regions as well as a water maser. The two HII regions are located at R.A. = 49^h707, Dec. = 45^m03 and R.A. = 49^h716, Dec. = 44^m13. Along with the multiple velocity components seen in this maser in the 2002 observations, this region of M82 is particularly interesting. Figure 8 shows this region in more detail. The location of this maser also appears to be on the edge of one of the H I/CO shells (Wills et al. 2002) and there is a 1720 MHz maser detection within a beam width.

The brightest X-ray source in M82 is located at 50^h2, 46^m7 (Kaaret et al. 2001) with a 1σ error circle of 0.7 arcseconds. None of the maser detections lie within this circle, the closest detection being 50.02+45.8 which lies at a distance of 2^m85 (a linear distance of 44 parsecs) so is clearly not associated.

The black hole candidate described by Ptak & Griffiths (1999) is located at R.A. = 09^h55^m52^s, Dec. = +69^o40'48" with a 1.3 arcminute diameter error circle. The nearest maser detection to this source is 51.87+48.3, a source only present in the 2002 data-set at 1665 MHz. The separation between these positions is 1^m9 so considering the uncertainties it is possible that they could be associated.

The AGN candidate suggested by Wills et al. (1997) and Seaquist et al. (1997) is spatially coincident with the

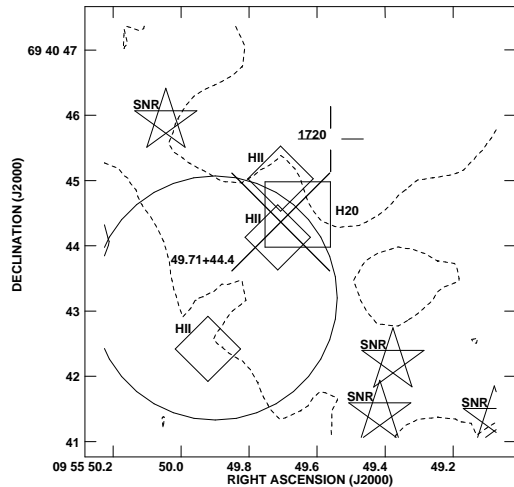


Figure 8. The region around 49.71+44.4 showing the OH absorption from the VLA 2002 observation (dotted lines), the HI shell (solid circle), HII regions (diamonds), water maser (square), supernovae (stars), 1720 MHz maser (broken plus) and the OH maser position from the 2002 data-set (cross). The symbols are $1''$ in size, apart from that for 49.71+44.4 which is the size of the restoring beam.

maser 52.71+45.8. This maser is apparently associated with an SNR, and one of only three detected at 1665 MHz while not detected at all at 1667 MHz. It is also the only one coincident with a satellite maser from Seaquist et al. (1997), a position which displayed absorption at 1720 MHz, but strong emission at 1612 MHz.

For completeness, Figure 9 shows the positions of the masers listed in Table 7 along with the positions of the HII regions and supernova remnants listed in McDonald et al. (2002), the satellite masers listed in Seaquist et al. (1997), the HI shells listed in Wills et al. (2002), H₂O masers from Baudry & Brouillet (1996), and the 2.2 μ m peak from Lester et al. (1990).

5.3 Comparison with other maser detections

The two brightest masers, 50.97+45.3 and 50.36+44.2, are coincident with the OH masers reported by Weliachew et al. (1984), corresponding to their masers m2 and m1 respectively. In their data, one source (labelled m1) is seen at 1665 MHz, while both their m1 and m2 are detected at 1667 MHz. In the 2002 VLA data, both masers are detected in both main lines at velocities of 80 and 98 ± 18 km s⁻¹ respectively. This is consistent with the velocities of the masers in Weliachew et al. (1984) where their m1 is at 65 to 80 km s⁻¹, and m2 has a velocity of 85 to 100 km s⁻¹.

Two of the OH masers reported here are apparently coincident with the H₂O features reported by Baudry & Brouillet (1996) to within the size of the $1''.4$ VLA beam in their observations. Their S2 is $0''.29$ from the MERLIN position of 50.97+45.3 while the brightest water maser, S3, lies $0''.63$ from the MERLIN position of 50.36+44.2. S1 and S4 from Baudry & Brouillet (1996) are both $>1''.6$ from the nearest MERLIN detection. One other

RA	Dec	S (mJy)
50 ^o 95	45 ^{''} 417	14.8
50.81	44.802	7.08
50.38	44.306	24.4

Table 6. List of the Gaussian components fitted to 50.97+45.3 and 50.36+44.2 for channel 47 in the VLA 2002 data. Each component had the same major and minor axis, and position angle as the restoring beam (1.34×1.31 at $23^\circ.19$).

OH maser, 49.71+44.4, is located $0''.57$ from a possible water maser detection listed by the same authors. The velocities of the H₂O masers are consistent (within the uncertainties) with those measured for the OH detections presented here, apart from perhaps 50.36+44.2/S3 although even here the difference is small: Baudry & Brouillet (1996) measure 103.9 km s⁻¹ for S3 where as 50.36+44.2 is found to have a velocity of 80 ± 18 km s⁻¹ from the 2002 VLA data.

Only one OH maser is coincident with a satellite line maser position reported by Seaquist et al. (1997): the separation of 52.71+45.8 with feature 4 from that paper (a feature seen in absorption at 1612 MHz but strong emission at 1720 MHz) is only $0''.57$. Both observations were carried out using the VLA with a $\theta_{\text{HPBW}} \sim 1''.4$. This position is also coincident with the SNR 44.01+59.6, one of three definite detections in this sample coincident with an SNR. Feature 4 in Seaquist et al. (1997) had a measured flux of 31.6 ± 1.7 mJy at 1612 MHz in 1996 November and a peak of only 1.98 mJy beam⁻¹ at 1665 MHz in 2002 November. At 1720 MHz there is no emission apparent, only an absorption feature is present at this position.

5.4 Spatial structure

Most of the masers are unresolved in the observations detailed here. This is not surprising given that the typical size of Galactic maser spots is much less than a parsec, considerably less than the resolution of the observations detailed here. One maser feature does show extension in the VLA data which resolves into two components when observed with MERLIN.

The extension to the SW of 50.97+45.3 in the VLA 2002 data-set can be seen in Figure 10. There is also a marginally detected second spatial component to this maser in the MERLIN 1995 data at the same position angle as the elongation seen in the 2002 data (see Figure 11), although it is only present at just over 3σ . The weak detection suggests that there is structure in the MERLIN data-set on scales larger than those to which the interferometer is sensitive which is resolved out. Using the AIPS task JM-FIT to fit Gaussian components to a region including masers 50.97+45.3 and 50.36+44.2 in the VLA 2002 data produces a better quality fit when three components are used, rather than two. The positions of the resulting fitted Gaussian components are given in Table 6.

The maser 49.71+44.4 appears to consist of multiple components at different velocities in the 1667 MHz line. This velocity structure is seen in the MERLIN 1995 and VLA 2002 data and may consist of multiple spatial components

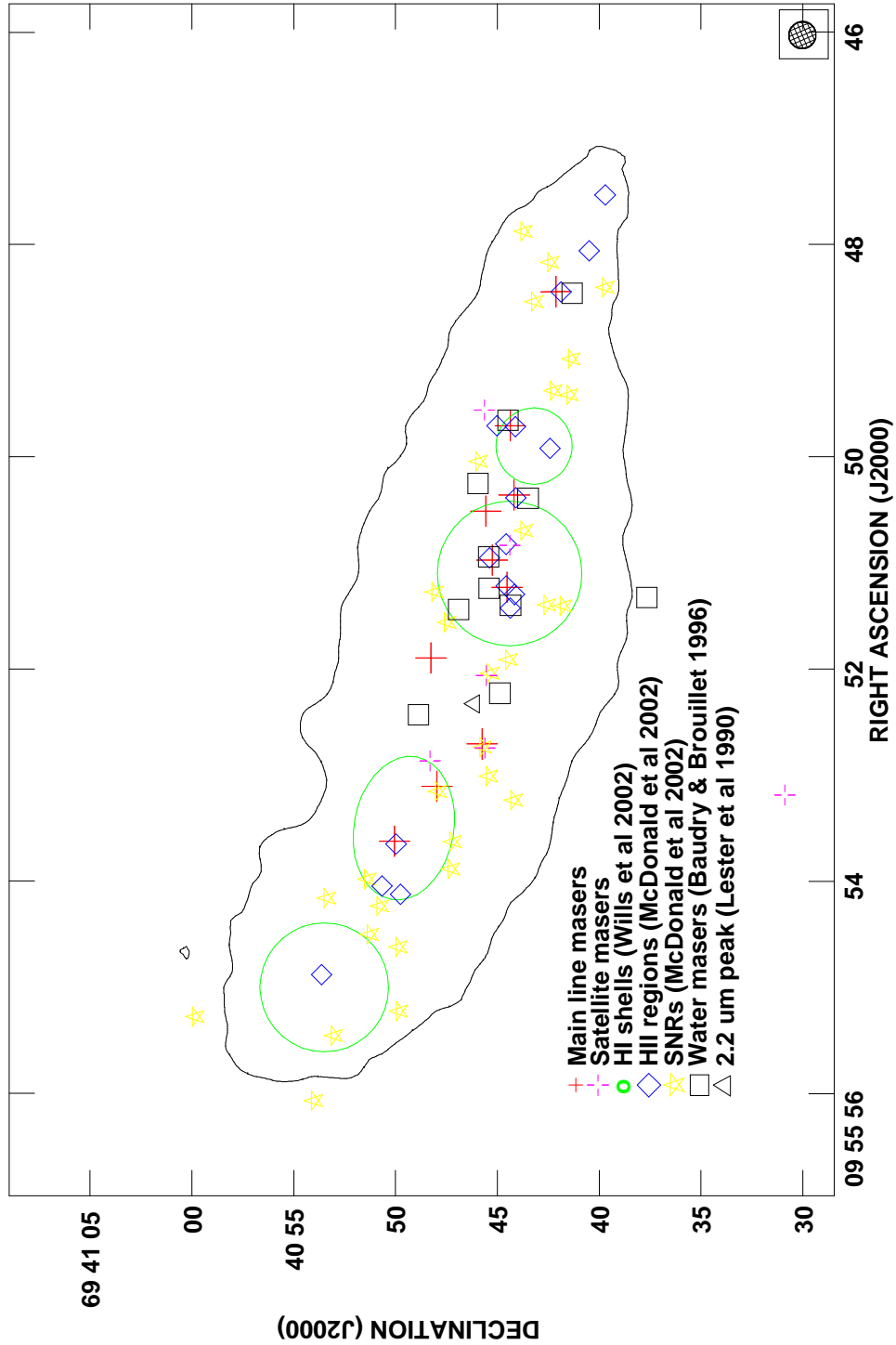


Figure 9. The location of the main line masers in M82 with other features shown for comparison. The solid line is a 1σ contour of the continuum emission from the VLA data cube. The full crosses mark the positions of the main line masers reported here. The crosses with gaps mark the 1612/1720 MHz masers reported in Seaquist et al. (1997). The diamonds and stars mark the HII regions and SNRs from McDonald et al. (2002) respectively.

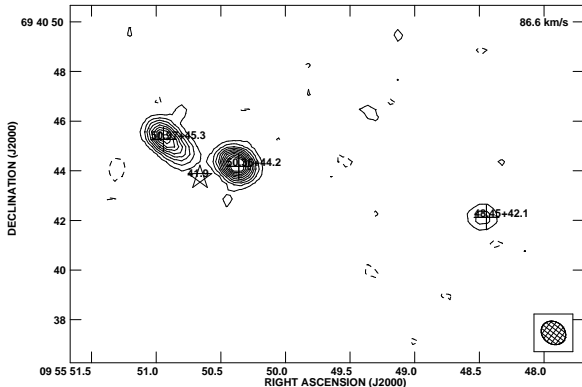


Figure 10. Three of the central masers in a continuum-subtracted single channel from the VLA 2002 data-set showing the extension of maser 50.97+45.3. The position of the brightest continuum feature (the SNR 41.9+57.5) is marked by a star. Contours are at $(-1, 1, 2, 3, 4, 5, 6, 7, 8, 9, 10) \times 1.751$ mJy/beam.

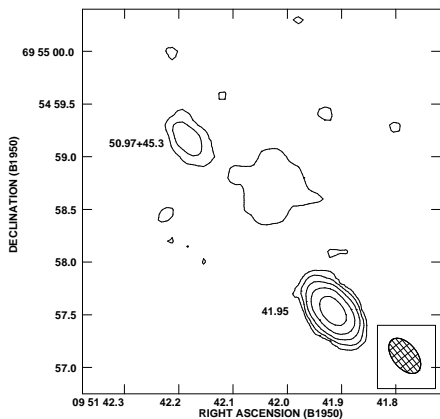


Figure 11. One of the central masers in a single channel from the MERLIN 1995 data-set showing the extension of maser 50.97+45.3. This image shows both the maser and continuum features. The position of the brightest continuum feature (the SNR 41.9+57.5) is toward the bottom of the image. Contours are at $(-1, 1, 2, 4, 8, 16, 32$ and $64) \times 2.6$ mJy/beam.

within a small region. This source is discussed in more detail in Section 5.5.

5.5 Velocity distribution

Figure 4 shows the spectra of the ten definite masers detected at greater than 5σ in the 2002 observations. Most of the masers are clearly visible above the absorption but it can be seen that others, like 49.71+44.4, may be hidden in the absorption. It can also be seen that while some of the masers have the same line-of-sight velocity as the underlying absorption, several are blue or red shifted slightly. The velocities of each feature measured in this data-set are given in Table 7.

The velocities measured for most of the masers lie on a line consistent with the rotation of a disk; this can be seen in

ID (J2000)	Velocity (km s ⁻¹)	Nearest continuum feature (B1950)
53.62+50.1	347±9	44.93+63.9 (HII)
53.11+48.0	281±9	44.43+61.8 (SNR)
52.71+45.8	233±9	44.01+59.6 (SNR)
51.87+48.3	238±9	-
51.23+44.5	119±9	42.48+58.4 (HII)
50.97+45.3	96±9	42.21+59.2 (HII)
50.51+45.6	203±9	-
50.36+44.2	79±9	41.64+57.9 (HII)
49.71+44.4	148±9	40.96+57.9 (HII)
48.45+42.1	107±9	39.68+55.6 (HII)

Table 7. The velocities of the ten definite maser detections in the VLA 2002 data. The features are named according to their J2000 positions (relative to 09^h55^m +69°40′). Velocities are measured with respect to the line rest velocity and where a maser is detected in both lines the velocities are consistent between the two. The nearest continuum features are from, and are labelled according to, the convention used in McDonald et al. (2002) (their corresponding J2000 IDs are given in Table 8).

Figure 12. The sources 53.62+50.1, 53.11+48.0, 52.71+45.8, 51.87+48.3 and 48.45+42.1 are at the same velocity as the OH absorption from the galaxy. On the other hand, 51.23+44.5, 50.97+45.3, 50.36+44.2 and 49.71+44.4 lie on an arc which is blue shifted with respect to the absorption at the same position. The location of this arc is coincident with the possible shell seen in CO emission by Matsushita et al. (2000) and HI absorption by Wills et al. (2002) (see Figure 13) and could be associated with a superbubble around the unusual source 41.95+57.5 (Muxlow et al. 2005). Figure 3 shows that there is little OH absorption around this position. Another possibility is that these features, rather than being associated with a bubble or shell-like feature, are situated on the line of the inner orbits of the possible bar structure described by Wills et al. (2000).

One of the masers associated with this velocity feature, 49.71+44.4 is unusual. In the VLA 2002 data-set there is an emission feature at 2.34 mJy in the 1667 MHz line with a velocity of 151 km s⁻¹. This feature has a weaker counterpart in the 1665 MHz line with a peak of <1 mJy at a velocity of 168 km s⁻¹. There also appears to be a possible very weak second emission feature in the 1667 MHz line with a velocity of 222 km s⁻¹. This second feature is comparable with the noise in the map so was initially ignored. However, this second component in the 1667 MHz line is also present in the MERLIN 1995 data.

6 COMPARISON WITH OTHER SURVEYS

Ball & Staelin (1968) compare OH maser detections at various frequencies with other objects. They find that HII regions are generally brightest in either of the main lines (class I in the terminology of Turner 1969) while those associated with SNRs or other non-thermal sources associated with HII regions are brightest at 1612 or 1720 MHz (Turner’s class II) and suggest that the processes in non-thermal sources could inhibit the main line emission.

In their conclusions, Pavlakis & Kylafis (1996) state that where both 1665 and 1667 MHz lines are spatially co-

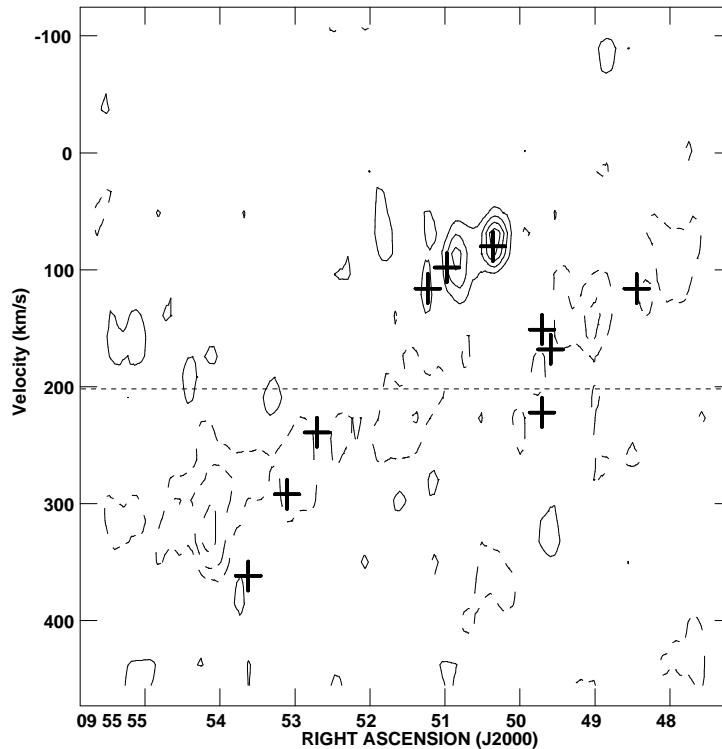


Figure 12. A comparison between the maser velocities and the absorption. Crosses represent measurements of maser velocities from the 2002 data. The contours represent the OH absorption (and emission) from the VLA 2002 dataset and the horizontal dashed line represents the systemic velocity of M82.

incident, an FIR radiation field (assumed to be due to thermal emission from dust) must be present. They also state that the 1665 MHz line is typically stronger than that at 1667 MHz. Most of the masers seen M82 appear to display the opposite behaviour, with the 1665 emission weaker, in most cases, than that at 1667 MHz.

A survey by Caswell (1998) of OH ground state masers in the Southern Galactic plane confirmed previous conclusions that the 1665 and 1667 MHz lines often occur together in space. The 1665 MHz line is usually stronger than the 1667 MHz line by a factor of around 3, although the 1667 MHz line is stronger in some sources by up to a factor of 4.

Caswell et al. (1980) survey a selection of the Galactic plane for OH in a restricted longitude range. They detect a total of 40 main line maser sources, most of which are brighter at 1665 than 1667 MHz. Most are also associated with known HII regions, while two of the eight remaining sources with no known HII associations may be associated with SNRs. Three of the masers in M82 are similarly associated with SNRs rather than HII regions, although the possibility that there are undetected HII regions along the same line of sight cannot be discounted.

Wilson & Barrett (1972) (and later Slotmaker et al. 1985) searched for OH masers associated with late-type stars in the Milky Way and found that most sources displaying emission in the main lines were brighter at 1667 MHz than at 1665 MHz. They find that a positive 1667:1665 brightness ratio appears to be more characteristic of evolved stars, rather than star formation and HII regions, with the differences in strength of emission due to the properties of the dust grains in the masing cloud (Elitzur 1992).

The most surprising result to come from this study is that, contrary to the results of other surveys discussed here, most of the masers in M82 are brighter at 1667 MHz and appear associated with HII regions. This would imply that most of these masers are associated with regions of evolved stars, rather than HII/OH regions as they appear to be. However, the apparent associations here are not necessarily physical and could just be due to line of sight coincidences since maser emission is the result of the amplification of background continuum emission. Another possibility is that, as the resolution of these observations is 3 pc at best, they are not physically associated with the observed HII regions but with nearby regions of evolved stars. Higher angular resolution measurements would be required in order to in-

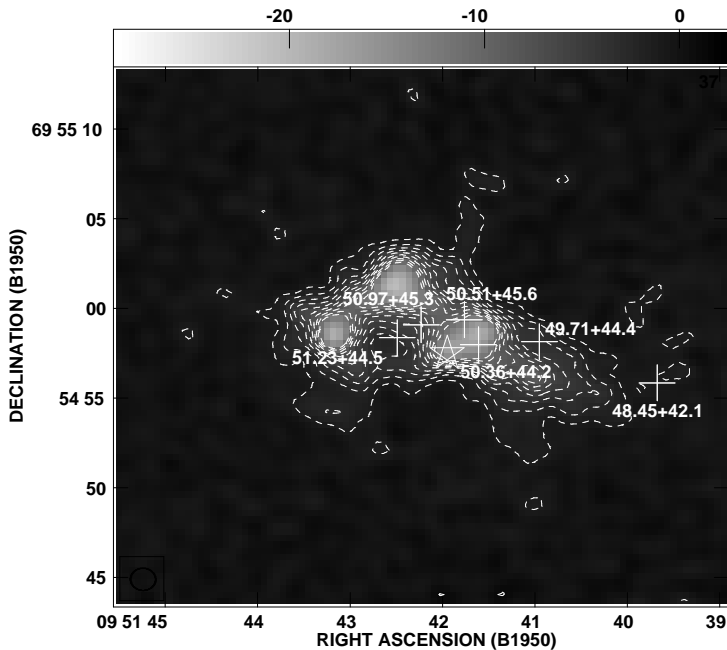


Figure 13. The positions of the masers in the centre of M82 in relation to the HI absorption shell seen by Wills et al. (2002) at a velocity of 173 km s^{-1} . Contours are of the HI absorption at $(-10 \text{ to } +10 \text{ in steps of } 1) \times 1.1 \text{ mJy/beam}$.

investigate whether the associations are real and physical, or just due to line-of-sight effects.

7 CONCLUSIONS

Nine new OH main line masers have been detected in the central starburst region of the nearby galaxy M82. On a position-velocity plot of the galaxy, most of the masers lie along the same axis as the gas. Four of the masers are blue-shifted from the main distribution and could possibly be on the edge of an expanding shell or caused by gas orbiting within a bar. Most appear associated with HII regions but are more characteristic of masers associated with late-type stars.

Due to the spectral resolution of the 2002 VLA observations the masers were not resolved in frequency, with most only visible in two channels. As the individual spots are an order of magnitude more luminous than typical Galactic masers, it is likely that they are made up of more than one individual masing region, so would have structure both spatially and in frequency. In order to investigate this further, observations have recently been made using the European VLBI Network in order to provide higher spatial resolution (much less than 1 pc at the distance of M82), and the VLA at higher spectral resolution. It is hoped that further investigation using these two observations will show evidence of both spatial and velocity structure.

It is likely that there are more main line OH masers in M82 but, due to the depth of absorption and the low velocity resolution, faint or narrow masers could be buried to the

extent that they are undetectable in the 2002 observations. The recent high spectral resolution VLA observations will have a gain in sensitivity over the 2002 observations which should enable the detection of weaker masers.

Most of the maser spots detected are unresolved and likely consist of large numbers of small masing clouds. Any variability could be due either to variability of a few strong sources in a particular spot, the creation/destruction of many weaker maser sources within a spot, or a combination of both.

The association of most maser features with HII regions is not surprising given the results of surveys carried out in our own Galaxy, although the comparative strength of the 1667 MHz line is more characteristic of late-type stars than HII regions. The association of two masers with known supernova remnants, while unusual, is not unique. A more sensitive survey for emission at 1612 and 1720 MHz would also help determine the nature of the maser sources.

Acknowledgements

MERLIN is run by the University of Manchester as a National Facility on behalf of PPARC. The VLA is operated by the National Radio Astronomy Observatory, a facility of the National Science Foundation operated under cooperative agreement by Associated Universities, Inc. MKA acknowledges support from a PPARC studentship. RJB acknowledges support from the European Commission's I3 programme "RADIONET" under contract 505818.

ID (J2000)	1995		1997		2002		Nearest feature (B1950)	Nearest feature (J2000)
	S ₁₆₆₅	S ₁₆₆₇	S ₁₆₆₅	S ₁₆₆₇	S ₁₆₆₅	S ₁₆₆₇		
53.62+50.1	<2.6	<2.6	<17	<18	2.44	2.49	44.93+63.9 (HII)	53.65+50.0
53.11+48.0	5.57	<2.6	<17	<18	1.86	<0.77	44.43+61.8 (SNR)	53.14+47.8
52.71+45.8	<2.6	<2.6	<17	<18	5.02	<0.77	44.01+59.6 (SNR)	52.73+45.7
51.87+48.3	<2.6	<2.6	<17	<18	1.71	<0.77	-	-
51.23+44.5	<2.6	<2.6	<17	<18	4.85	5.93	42.48+58.4 (HII)	51.22+44.5
50.97+45.3	8.35	7.83	<17	23.0	13.0	18.5	42.21+59.2 (HII)	50.95+45.2
50.51+45.6	<2.6	<2.6	<17	<18	1.85	1.28	-	-
50.36+44.2	7.01	29.9	<17	57.2	10.7	50.5	41.64+57.9 (HII)	50.39+44.1
50.02+45.8	4.30	5.09	<17	<18	<0.77	<0.77	41.29+59.7 (SNR)	50.06+45.9
49.71+44.4	<2.6	5.29	<17	<18	<0.77	2.34	40.96+57.9? (HII)	49.71+44.1
48.45+42.1	4.15	6.94	<17	<18	2.64	5.97	39.68+55.6 (HII)	48.44+41.9

Table 8. All masers detected in the data-sets discussed here. Fluxes are given for each masers in each line in which it was detected in each epoch, along with the closest continuum feature from McDonald et al. (2002) given in both B1950 and J2000 coordinates.

REFERENCES

- Baan W. A., Wood P. A. D., Haschick A. D., 1982, *Astrophys. J. Letters*, 260, L49
- Ball J. A., Staelin D. H., 1968, *Astrophys. J. Letters*, 153, L41+
- Baudry A., Brouillet N., 1996, *Astron. Astrophys.*, 316, 188
- Caswell J. L., 1998, *Mon. Not. R. Astr. Soc.*, 297, 215
- Caswell J. L., Haynes R. F., Goss W. M., 1980, *Australian Journal of Physics*, 33, 639
- Elitzur M., 1992, *Astronomical masers. Astronomical masers Kluwer Academic Publishers (Astrophysics and Space Science Library. Vol. 170)*, 365 p.
- Freedman W. L., Hughes S. M., Madore B. F., Mould J. R., Lee M. G., Stetson P., Kennicutt R. C., Turner A., Ferrarese L., Ford H., Graham J. A., Hill R., Hoessel J. G., Huchra J., Illingworth G. D., 1994, *Astrophys. J.*, 427, 628
- Hagiwara Y., 2005, *Astrophysics and Space Science*, 295, 125
- Hagiwara Y., Henkel C., Menten K. M., Nakai N., 2001, *Astrophys. J. Letters*, 560, L37
- Henkel C., Wilson T. L., 1990, *Astron. Astrophys.*, 229, 431
- Kaaret P., Prestwich A. H., Zezas A., Murray S. S., Kim D.-W., Kilgard R. E., Schlegel E. M., Ward M. J., 2001, *Mon. Not. R. Astr. Soc.*, 321, L29
- Kronberg P. P., Wilkinson P. N., 1975, *Astrophys. J.*, 200, 430
- Lester D. F., Gaffney N., Carr J. S., Joy M., 1990, *Astrophys. J.*, 352, 544
- Matsushita S., Kawabe R., Matsumoto H., Tsuru T. G., Kohno K., Morita K.-I., Okumura S. K., Vila-Vilaró B., 2000, *Astrophys. J. Letters*, 545, L107
- McDonald A. R., Muxlow T. W. B., Wills K. A., Pedlar A., Beswick R. J., 2002, *Mon. Not. R. Astr. Soc.*, 334, 912
- Minier V., Booth R. S., Conway J. E., 2002, *Astron. Astrophys.*, 383, 614
- Muxlow T. W. B., Pedlar A., Beswick R. J., Argo M. K., O'Brien T. J., Fenech D., Trotman W., 2005, *Memorie della Societa Astronomica Italiana*, 76, 586
- Nguyen-Q-Rieu, Mebold U., Winnberg A., Guibert J., Booth R., 1976, *Astron. Astrophys.*, 52, 467
- Pavlakis K. G., Kylafis N. D., 1996, *Astrophys. J.*, 467, 309
- Ptak A., Griffiths R., 1999, *Astrophys. J. Letters*, 517, L85
- Seaquist E. R., Frayer D. T., Frail D. A., 1997, *Astrophys. J.*, 487, L131
- Shen J., Lo K. Y., 1995, *Astrophys. J. Letters*, 445, L99
- Slotmaker A., Habing H. J., Herman J., 1985, *Astronomy and Astrophysics Supplement Series*, 59, 465
- Turner B. E., 1969, *Astrophys. J.*, 157, 103
- Weliachew L., Fomalont E. B., Greisen E. W., 1984, *Astron. Astrophys.*, 137, 355
- Wills K. A., Das M., Pedlar A., Muxlow T. W. B., Robinson T. G., 2000, *Mon. Not. R. Astr. Soc.*, 316, 33
- Wills K. A., Pedlar A., Muxlow T. W. B., 2002, *Mon. Not. R. Astr. Soc.*, 331, 313
- Wills K. A., Pedlar A., Muxlow T. W. B., Wilkinson P. N., 1997, *Mon. Not. R. Astr. Soc.*, 291, 517
- Wilson W. J., Barrett A. H., 1972, *Astron. Astrophys.*, 17, 385